Article

Neuron

Feeding State Modulates Behavioral Choice and Processing of Prey Stimuli in the Zebrafish Tectum

Highlights

- Feeding state influences approach versus avoidance decisions in zebrafish
- Hunger alters the neural representation of prey-like stimuli in the tectum
- The neuroendocrine and serotonergic systems mediate the modulation by feeding state

Authors

Alessandro Filosa, Alison J. Barker, Marco Dal Maschio, Herwig Baier

Correspondence

hbaier@neuro.mpg.de

In Brief

Filosa et al. show that hunger enhances the decision by larval zebrafish to approach (versus avoid) moving visual objects and the processing of prey cues in the tectum through signals from the hypothalamic-pituitary-interrenal axis and serotonergic system.

Filosa et al., 2016, Neuron *90*, 596–608
May 4, 2016
http://dx.doi.org/10.1016/j.neuron.2016.03.014

CellPress

CellPress

Neuron
Article

Feeding State Modulates Behavioral Choice and Processing of Prey Stimuli in the Zebrafish Tectum

Alessandro Filosa,[1] Alison J. Barker,[1] Marco Dal Maschio,[1] and Herwig Baier[1,*]
[1]Max Planck Institute of Neurobiology, Am Klopferspitz 18, 82152 Martinsried, Germany
*Correspondence: hbaier@neuro.mpg.de
http://dx.doi.org/10.1016/j.neuron.2016.03.014

SUMMARY

Animals use the sense of vision to scan their environment, respond to threats, and locate food sources. The neural computations underlying the selection of a particular behavior, such as escape or approach, require flexibility to balance potential costs and benefits for survival. For example, avoiding novel visual objects reduces predation risk but negatively affects foraging success. Zebrafish larvae approach small, moving objects ("prey") and avoid large, looming objects ("predators"). We found that this binary classification of objects by size is strongly influenced by feeding state. Hunger shifts behavioral decisions from avoidance to approach and recruits additional prey-responsive neurons in the tectum, the main visual processing center. Both behavior and tectal function are modulated by signals from the hypothalamic-pituitary-interrenal axis and the serotonergic system. Our study has revealed a neuroendocrine mechanism that modulates the perception of food and the willingness to take risks in foraging decisions.

INTRODUCTION

Animals constantly face choices influencing their well-being and survival. Decision making has emerged as a central theme in neuroeconomics and neuroethology (Kristan, 2008; Pearson et al., 2014). The notion that animals base their decisions solely on the absolute values of the alternatives has been challenged by concepts originally derived from behavioral economics (Kahneman and Tversky, 1979; Symmonds et al., 2010). For example, in order to survive, animals need to escape from threats and move toward food sources. Clearly, escape versus approach decisions need to be flexible and to consider the costs and benefits of their outcome. This is because, in complex environments, animals often face a trade-off between acquiring resources and becoming a resource for others (Lima and Dill, 1990). A hungry animal may, therefore, increase its predation risk to avoid starvation.

Studies in invertebrates showed that hunger is capable of modulating the processing of sensory inputs and simple behaviors, such as odor- and taste-dependent approaches toward food sources (Bargmann, 2012; Bräcker et al., 2013; Hirayama and Gillette, 2012; Inagaki et al., 2014; Longden et al., 2014; Marella et al., 2012; Palmer and Kristan, 2011). However, the neural circuits mediating the effects of appetitive states on sensorimotor decision making are still not completely understood. Moreover, the impact of this type of modulation on other sensory modalities, such as vision, and more complex behaviors in vertebrates remains largely unknown.

Here, we investigated the neural mechanism underlying behavioral responses to ambiguous visual stimuli using the zebrafish, a versatile vertebrate model organism amenable to genetic manipulations and optical probing (Baier and Scott, 2009). Our behavioral assay measures the decision of zebrafish larvae to avoid or approach moving objects of various sizes. In a previous study, we established that this decision is biased by stimulus size (Barker and Baier, 2015). Small black circles, drifting in the visual field below the fish, elicited mostly prey-capture swims, while large black circles reliably evoked escapes. Thus, the pursuit of small but potentially ambiguous stimuli serves as a proxy measure of risk-prone behavior. We now show that this behavior is strongly affected by feeding state. Hungry animals pursued small objects more often than fed fish and escaped less often from larger ones. We further demonstrate, with optical imaging, that starvation results in an expanded representation of small, prey-like objects in the tectum, the homolog of the mammalian superior colliculus. We found that the hypothalamic-pituitary-interrenal (HPI) axis and the serotonergic system mediate the effects of hunger on behavior and tectal activity. Our results reveal a modulatory mechanism by which feeding state influences the visual perception of food and the willingness to take risks in foraging decisions.

RESULTS

Hunger Modulates Behavioral Choice in an Approach versus Avoidance Assay

Food items are generally smaller than predators. Therefore, size categorization is an efficient way for an animal to make a quick decision to either pursue or avoid an unknown object (Ewert, 1970). We used a size-discrimination assay to test the effects of feeding state on visually driven approach versus avoidance decision making in zebrafish larvae (Barker and Baier, 2015) (Figure 1A). We used two different metrics to analyze interactions

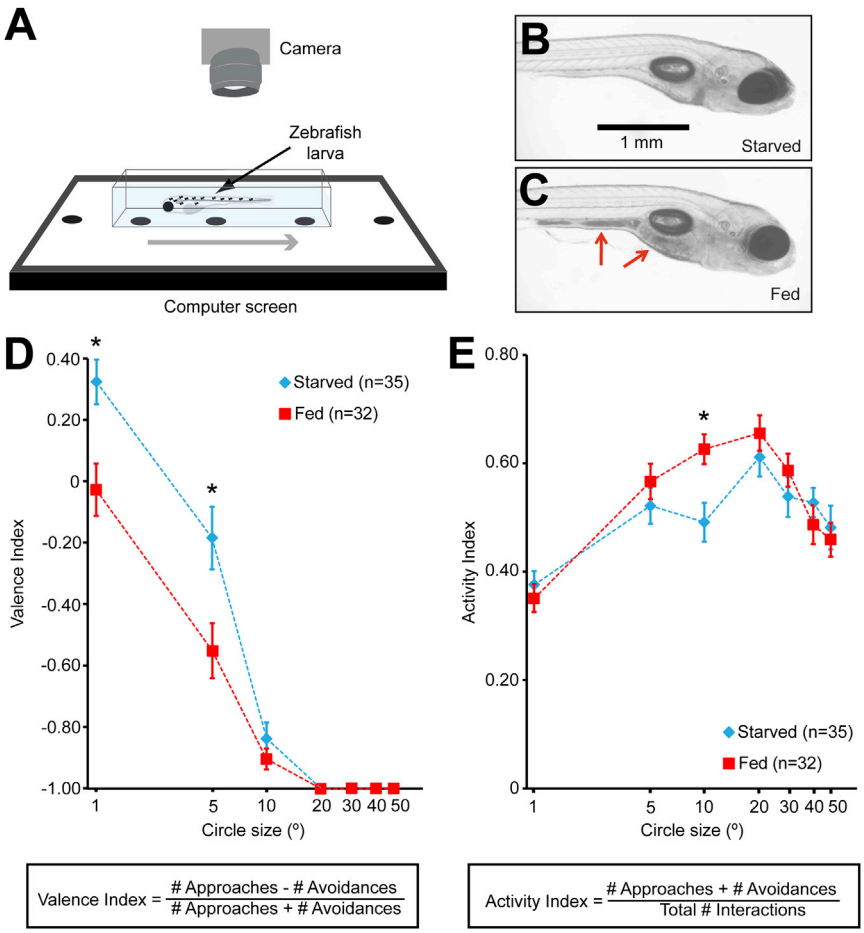

Figure 1. Decision between Approach versus Avoidance Is Modulated by Feeding State

(A) Scheme of the behavioral setup.

(B and C) Examples of starved (B) and fed (C) 7 dpf zebrafish larvae demonstrating easy identification of individuals with food in their digestive tract (red arrows).

(D and E) Graphs depicting average valence (D) and activity (E) indeces of starved and fed 7 dpf larvae for various stimulus sizes (plotted on logarithmic scale). The valence index measures the tendency of animals to either pursue (positive valence) or avoid (negative valence) visual stimuli, without considering pursuit and avoidance efficiency. When the visual index is 0, larvae pursue or avoid circles with a 50% probability. The fish-visual stimulus interaction efficiency is measured with the activity index. *$p < 0.05$; t test with Benjamini-Hochberg correction. Data are presented as mean ± SEM. See also Movies S1 and S2.

between fish and visual stimuli. The valence index measures the tendency of animals to either approach (positive valence) or avoid (negative valence) visual stimuli, without considering neutral interactions (see formula in Figure 1). When the valence index is zero, larvae pursue or avoid circles with a 50% probability. The activity index, by taking in consideration also neutral interactions, measures the probability of a fish to react to a visual stimulus, with either an approach or avoidance (see formula in Figure 1). Consistent with the earlier study, small circles mainly elicited approaches, often including pursuits, while large circles evoked escapes, consisting of rapid turns away from the stimulus (Movies S1 and S2).

Zebrafish embryos use their yolk as an energy reservoir. However, this is depleted by 6 days post-fertilization (dpf), and larvae have to actively search for food to survive (Kimmel et al., 1995). We supplied one group of larvae with food, starting at 6 dpf, while another group was not fed (Figures 1B and 1C). We measured the pH and osmolarity of the medium to rule out alterations of its chemico-physical properties by the addition of food (Table S1). Notably, we found that starved larvae performed more pursuits and fewer escapes in the presence of small circles at 7 dpf, compared to fed controls (Figure 1D). They were also less likely than fed fish to escape from circles of intermediate size (Figure 1E). We interpreted these results as a starvation-driven reduction of aversive behavior.

The HPI Axis Adjusts Behavioral Choice to the Animal's Energy Needs

The hypothalamic-pituitary-adrenal (HPA) axis, which, in teleost fish, is called the HPI axis, is a neuroendocrine pathway regulating defensive behaviors in response to threats (Ulrich-Lai and Herman, 2009). Its anatomical and molecular features are highly conserved among vertebrates (Alderman and Bernier, 2009; Löhr and Hammerschmidt, 2011), including the peptides corticotropin-releasing hormone (CRH) and adrenocorticotropic hormone (ACTH) and the glucocorticoid cortisol (Figure 2A). Binding of cortisol to glucocorticoid receptors (GRs) mediates negative feedback on CRH and ACTH production (Ziv et al., 2013). We hypothesized that the reduction of aversive behavior in starved zebrafish could be mediated by reduced activity of the HPI axis induced by lack of food intake. For this reason, we measured the amount of cortisol in starved and fed larvae. Remarkably, we observed a strong reduction of cortisol levels in starved animals, compared to satiated ones (Figure 2B). This result argues that HPI axis activity is inversely correlated with the animal's energy needs.

In order to test the link between HPI axis activation and regulation of visual behavior, we took advantage of a mutant with elevated HPI axis activity. In $gr^{s357/s357}$ homozygous mutants (Ziv et al., 2013), a missense mutation in the DNA-binding domain of the GR abolishes transcriptional activity of this protein and, consequently, eliminates the cortisol-mediated negative feedback on the HPI axis (Figure 2A). As a consequence, $gr^{s357/s357}$ homozygous fish show a chronically elevated HPI axis, including higher concentrations of CRH, ACTH, and cortisol (Griffiths et al., 2012; Ziv et al., 2013). As predicted, increasing the activity of the HPI axis mimicked the effect of feeding on behavioral performance in the size-discrimination assay. Mutant larvae assigned a more negative valence to small visual stimuli,

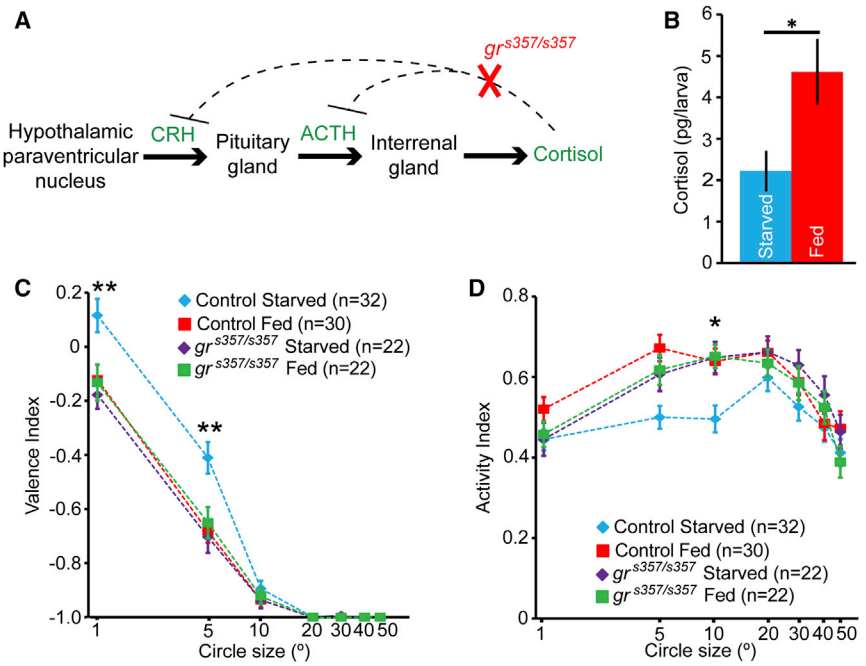

Figure 2. The Effect of Feeding State on Behavioral Choice Is Mediated by the HPI Axis

(A) Scheme of the HPI axis. In $gr^{s357/s357}$ mutants the cortisol-mediated negative feedback on the HPI axis is impaired.

(B) Average cortisol amounts in starved and fed 7 dpf larvae. n = 7 groups of 24 larvae per condition, *p = 0.02, t test.

(C and D) Graphs depicting valence (C) and activity (D) indices (plotted on logarithmic scale) of $gr^{s357/s357}$ and control larvae. *p < 0.05; **p < 0.01, t test with Benjamini-Hochberg correction. Asterisks indicate statistical significance only for the control starved and $gr^{s357/s357}$ starved comparison. Data are presented as mean ± SEM.

See also Table S2.

pursuing them less or avoiding them more than control starved animals (Figures 2C and 2D; Tables S2A and S2B). Moreover, the effect of food intake on behavior performance was occluded in mutant fish (Figures 2C and 2D), suggesting that the HPI axis regulates behavioral choice downstream of, and not parallel to, metabolic signals.

Serotonin Mediates the Effect of Hunger on Behavioral Choice

Since the HPA axis is a well-known regulator of the serotonergic system (Fox and Lowry, 2013), we tested the hypothesis that serotonin could modulate behavioral choice. First, we measured the activity of serotonergic neurons in the raphe nucleus, a known target of the HPI axis (Fox and Lowry, 2013), of fed and starved 7 dpf *tph2:Gal4ff, UAS:GFP* larvae, in which serotonergic neurons are labeled with GFP (Yokogawa et al., 2012). We used immunofluorescence detection of phosphorylated extracellular-signal-regulated kinase (pERK) as a time-averaged readout of neuronal activity (Figures 3A–3C). ERK is phosphorylated following neuronal depolarization (Rosen et al., 1994), and the amount of pERK in a neuron is positively correlated with neuronal activity (Randlett et al., 2015). Interestingly, we found that the cell bodies of raphe serotonergic neurons contained higher amounts of pERK in starved than fed larvae (Figure 3D), suggesting that hunger increases the activity of these neurons.

To test whether serotonin could modulate behavioral choice downstream of satiety signals, we analyzed the behavior of larvae treated with the selective serotonin reuptake inhibitor fluoxetine. Increasing serotonergic transmission in fed fish, by applying 1.5 μM fluoxetine for 4 to 5 hr, was sufficient to abolish the effect of food intake on behavioral performance (Figures 3E and 3F; Tables S2C and S2D). In a complementary set of experiments, we ablated serotonergic neurons with the enzyme nitroreductase (NTR) in *tph2:Gal4ff, UAS:ntr-mCherry* fish. NTR converts the innocuous drug metronidazole (MTZ) to its toxic form, killing the cells expressing the enzyme (Pisharath et al., 2007). Hungry larvae lacking serotonergic neurons behaved similarly to fed fish, assigning more negative valence to small visual stimuli, compared to hungry controls with an intact serotonergic system (Figure 3G). Ablation of serotonergic neurons did not alter the behavior of fed animals (Figure S1A), showing that the effects of the two manipulations were not additive and suggesting that satiety signals and serotonergic transmission are components of the same modulatory pathway. We did not observe differences in avoidance performance for circles of intermediate size (Figures 3H and S1B), possibly due to the involvement of some of the ablated serotonergic neurons in regulating general responsiveness of fish to visual stimuli. Together, these results suggest that the serotonergic system acts downstream of metabolic signals to modulate behavioral choice.

Feeding State Alters the Neural Responses to Visual Objects in the Tectum

Next, we investigated the impact of feeding state on neural circuits processing sensory stimuli. We focused our attention on the tectum, the main visual area in the fish brain (Nevin et al., 2010). In zebrafish, the tectum is required for hunting behavior (Gahtan et al., 2005) and avoidance of looming visual stimuli (Temizer et al., 2015). It is anatomically subdivided into a neuropil region, containing retinal ganglion cell (RGC) axons and neurites of periventricular neurons (PVNs), as well as a periventricular layer (PVL), containing the cell bodies of PVNs (Figure 4A). We used two-photon calcium imaging to analyze the effect of feeding state on the size selectivity of PVNs in the tectum of 7 dpf *elavl3:Gal4, UAS:GCaMP5* fish, expressing the genetically encoded calcium indicator GCaMP5 in the majority of neurons (Figures 4A and 4B). By showing moving black circles to the fish, we observed that tectal PVNs were tuned to a variety of visual stimulus sizes (Figure 4C), confirming previous studies (Barker and Baier, 2015; Niell and Smith, 2005; Preuss et al., 2014).

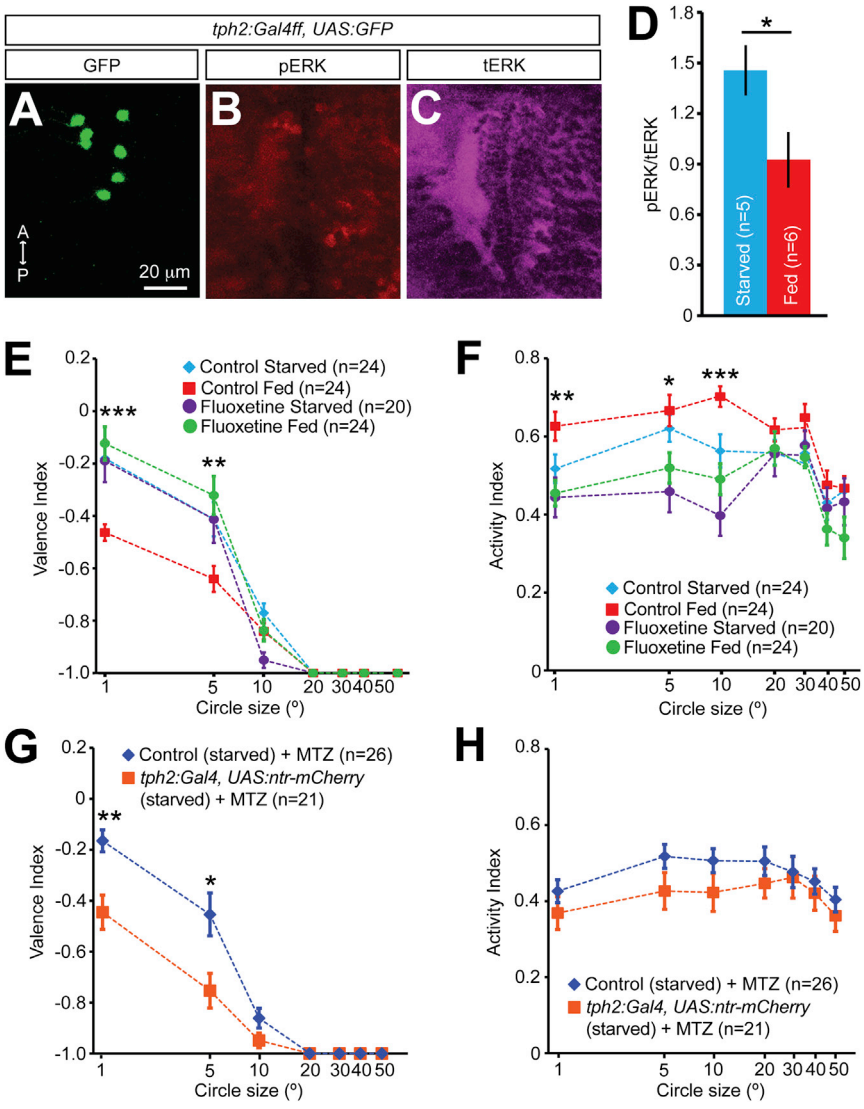

Figure 3. Serotonin Modulates Behavioral Choice Downstream of Feeding State

(A–C) Confocal images of a 7 dpf *tph2:Gal4ff, UAS:GFP* larva showing serotonergic neurons in the raphe nucleus (A), and immunofluorescence detection of phosphorylated ERK (pERK, B) and total ERK (tERK, C). A, anterior; P, posterior.

(D) Plot showing average pERK/tERK staining intensity ratios in raphe serotonergic neurons of 7 dpf fed or starved larvae. *p = 0.04, t test.

(E and F) Plots showing valence (E) and activity (F) indices of starved and fed larvae, treated with 1.5 μM fluoxetine, and untreated controls. *p < 0.05; **p < 0.01; ***p < 0.001, t test with Benjamini-Hochberg correction. Asterisks indicate statistical significance only for the control fed and fluoxetine fed comparison. Statistical results are summarized in Table S2.

(G and H) Graphs depicting valence (G) and activity (H) indices for fish lacking serotonergic neurons, and control larvae. *p < 0.05; **p < 0.01, t test with Benjamini-Hochberg correction. Data are presented as mean ± SEM.

See also Table S2.

In order to derive a metric to describe the tuning of each PVN to different stimulus sizes, we determined the weighted mean response (WMR) angle by calculating the weighted sums of visual stimulus sizes to which Ca^{2+} responses were non-zero, with weights corresponding to the relative ΔF/F values for each response (Figure 4D; Experimental Procedures). In this way, we could plot the size tuning of the entire tectal PVN population in the form of a cumulative distribution (Figure 4E). Remarkably, feeding state strongly influenced the visual size response properties of tectal neurons. The PVN population response of starved larvae was significantly shifted toward small, prey-like, visual stimuli, compared to the response of fed fish (Figure 4E). Control experiments showed that food odor alone was not responsible for the altered neural responses (Figure 4F).

Next, we tested whether hunger modulates neuronal activity in the tectum presynaptically at the level of RGC axons or postsynaptically on PVNs. Pixel-wise analysis of calcium signals in the tectal neuropil of 7 dpf *Isl2b:Gal4, UAS:GCaMP6s* larvae did not reveal macroscopic changes in the activity of RGC presynaptic terminals (Figures 5A–5C; Figure S2). These data demonstrate that hunger can have a strong impact on visual processing of food-related cues in the tectal circuitry downstream of RGCs.

Hunger Modifies the Activity of Specific Populations of Neurons in the Tectum

The *elavl3:Gal4* driver line includes in its expression pattern most neurons regardless of function, morphology, or transmitter identity. To gain more insight into the tectal network components regulated by feeding state, we analyzed the activity of genetically labeled neuron subtypes. First, we used 7 dpf *gad1b:Gal4, UAS:GCaMP6s* larvae to monitor the visual response properties of GABAergic cells (Figure 6A). We found that starvation induced a shift of GABAergic responses toward small, prey-like, visual stimuli (Figure 6B), suggesting that activity of GABAergic neurons is modulated by hunger.

We asked whether other types of tectal neurons were also modulated by feeding state. The gene-trap line *Gal4mpn354* drives expression of Gal4 in a small subpopulation of non-stratified PVNs, most of which are glutamatergic (Barker and Baier, 2015) (Figure 6C). Previous work strongly suggested that the activity of these neurons enhances approach behavior toward small visual stimuli (Barker and Baier, 2015). We found that starvation increased the number of *Gal4mpn354* PVNs tuned to small visual stimuli (Figures 6D and S3), suggesting that this subpopulation may be involved in adapting visual processing of prey-like cues and behavioral choice to the fish's energy needs. We did not detect any effect of feeding state

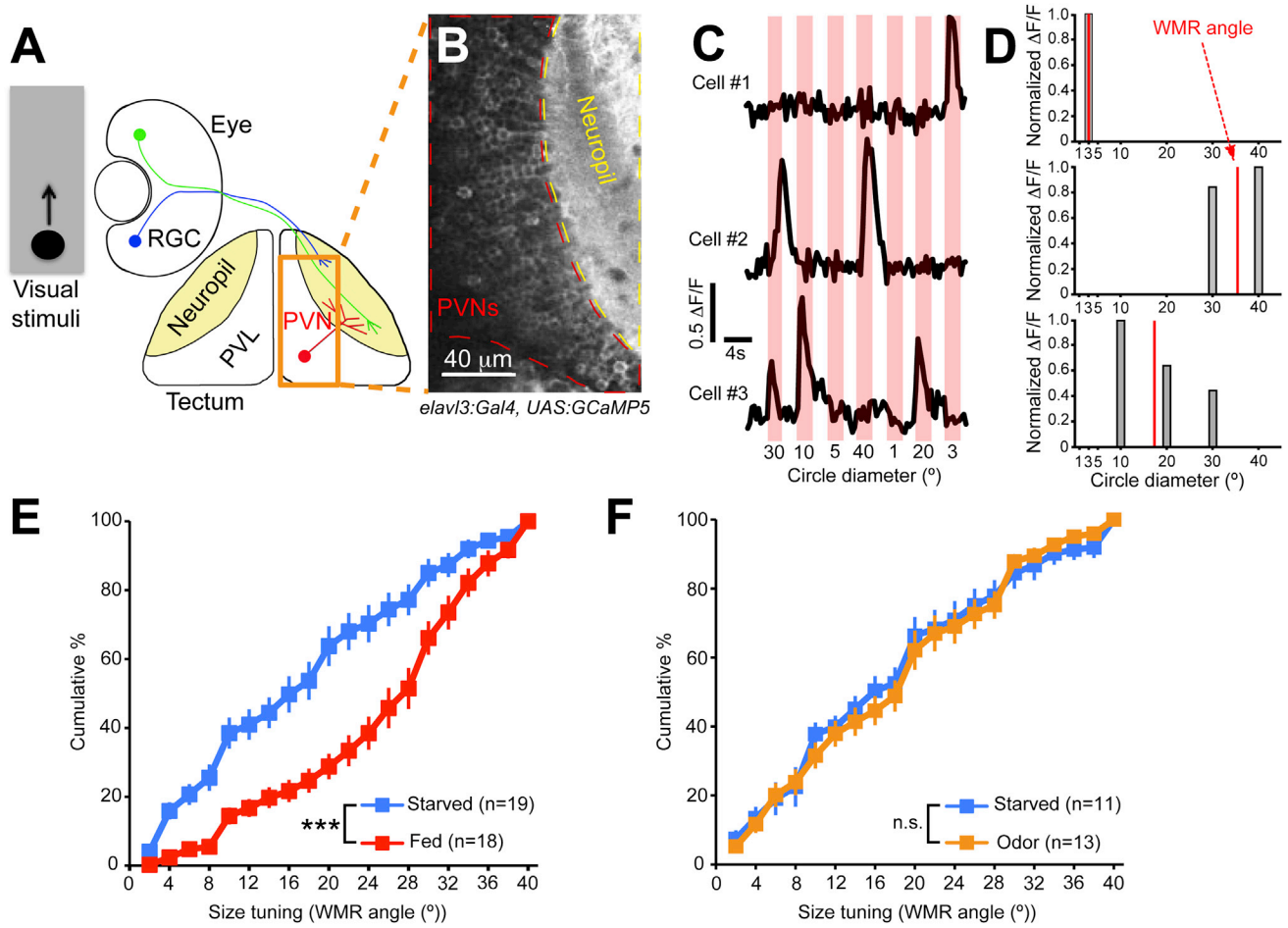

Figure 4. Feeding State Affects Visual Information Processing in the Tectum

(A) Scheme of the zebrafish retinotectal circuit and experimental setup.

(B) Two-photon image of the region of the tectum of a 7 dpf *elavl3:Gal4, UAS:GCaMP5* larva used for imaging.

(C) ΔF/F traces of PVNs responsive to different visual stimulus sizes. Vertical red bars indicate the presence of visual stimuli.

(D) Normalized ΔF/F values (gray bars) obtained from the PVN responses shown in (C) and the corresponding WMR angles (vertical red lines).

(E and F) Graphs comparing cumulative percentages of WMR angles for PVNs in starved and fed (E) or starved and starved + odor-exposed (F) 7 dpf *elavl3:Gal4, UAS:GCaMP5* larvae. ***p = 1.9E−16; n.s., not significant (two-sample Kolmogorov-Smirnov test). Data are presented as mean ± SEM.

on a subpopulation of PVNs labeled in the enhancer-trap line *Gal4s1038t* (Figures 6E and 6F). Interestingly, previous work had shown that these neurons were not involved in behavioral choice when fish were presented with small visual stimuli (Barker and Baier, 2015). Taken together, these data point to a modulatory effect of hunger on tectal GABAergic neurons and, in addition, show that a genetically defined population of neurons regulating approach behavior is also under control of metabolic signals.

The HPI Axis and the Serotonergic System Modulate Visual Size Representation in the Tectum

To test whether feeding state modulates processing of small visual stimuli in the tectum and behavioral choice through shared mechanisms, we first analyzed visual size response properties of PVNs in *elavl3:Gal4, UAS:GCaMP5, gr*$^{s357/s357}$ and control *elavl3:Gal4, UAS:GCaMP5, gr*$^{+/+}$ larvae. Similarly to fed larvae, and consistent with their behavioral phenotype, *gr*$^{s357/s357}$ fish showed a shift of the PVN population response toward larger visual stimuli (Figure 7A). Next, encouraged by the observation that the tectal neuropil is densely innervated by serotonergic neurites (Yokogawa et al., 2012) (Figures 7B–7D), we investigated whether serotonin could alter size representation in the tectum. We found that indeed, in a manner similar to its effect on behavior, the application of 1.5 µM fluoxetine abolished the effect of food intake on PVN responses (Figure 7E). These results suggest that reduced HPI axis activity and enhanced serotonergic transmission promote the starvation-induced shift of PVN responses toward small visual stimuli.

Serotonin Recruits Additional Tectal Neurons Tuned to Small Visual Stimuli

Hunger may change the population responses of tectal neurons in three ways: (1) tuning of individual neurons could change from

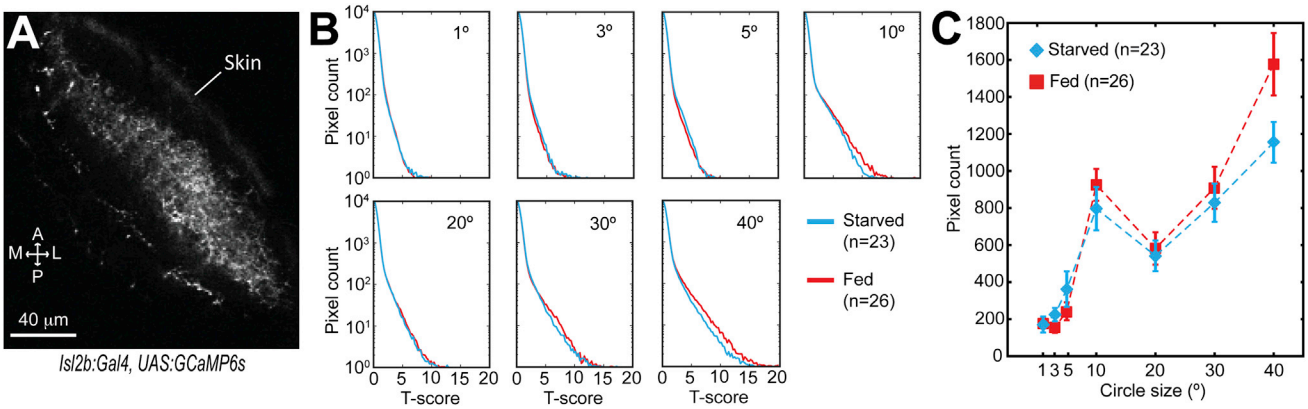

Figure 5. The Influence of Feeding State Is Not Detectable in RGC Axons in the Tectal Neuropil

(A) Two-photon image of the tectal neuropil of a 7 dpf *Isl2b:Gal4, UAS:GCaMP6s* larva showing RGC axons. A, anterior; L, lateral; M, medial; P, posterior.

(B) Average distributions of the T scores obtained from the pixel-wise analysis of the activity of RGC axons, in response to visual stimuli of different sizes (in degrees of visual angle) in fed or starved 7 dpf *Isl2b:Gal4, UAS:GCaMP6s* larvae. The procedure for calculating the T scores is summarized in Figure S2.

(C) Average numbers of pixels active in response to visual stimuli of different sizes. Background noise was removed by subtraction of a component related to image time series obtained in the absence of visual stimulation (see Experimental Procedures for details). Error bars represent SEM. No statistically significant differences were detected between fed and starved animals (t test with Benjamini-Hochberg correction). n = number of trials.

See also Figure S2.

large to small size preference, (2) additional neurons tuned to small sizes might be activated, or (3) neurons normally responsive to large sizes might be suppressed. We designed an experiment to distinguish between these possibilities, taking advantage of the fact that fluoxetine induces a starvation-like population response shift in the tectum of fed larvae. We first imaged visual responses of PVNs in fed 7 dpf *elavl3:Gal4, UAS:GCaMP5* larvae. We then applied 1.5 μM fluoxetine (or only fish water as a control) and recorded the activity of the same neurons again 3.5–4 hr later (Figures 8A and 8B).

We found that some neurons were active during both imaging sessions ("persistent"). However other neurons were active only before ("lost") or after ("gained") drug application (Figures 8A–8C). While the percentages of persistent neurons were similar in fluoxetine-treated fish and controls, the relative amounts of lost and gained neurons differed (Figure 8C). In control fish, there was a larger number of lost PVNs. In contrast, in fluoxetine-treated larvae, there were more gained PVNs. While the loss of active neurons in control larvae may be the consequence of stress caused by prolonged restraint of the fish in agarose, the presence of newly responsive neurons after fluoxetine application points to the activation of new populations of neurons that were silent in untreated, fed animals.

Next, we investigated whether the "gained" population contained a larger proportion of cells responsive to small visual stimuli compared to the "lost" population. This was, indeed, the case (Figure 8D), suggesting a net gain of neurons tuned to small stimuli. Control larvae showed the opposite, although not statistically significant, trend. We also found that fluoxetine did not change the tuning properties of persistent neurons (Figures 8E and S4). These data suggest a model in which serotonin mediates the effects of starvation on tectal function by activating PVNs tuned to small stimuli, with no significant alterations of size tuning in individual neurons.

DISCUSSION

We found that food-deprived zebrafish larvae displayed a stronger preference for small and intermediately sized stimuli, representing potentially edible items, than fed animals. These results cannot be interpreted as a simple decrease in interest of a fed larva for food-like items or a shift of the size preference since, in these cases, we should have observed an overall decrease of activity in response to small stimuli. The altered (more negative) values of the valence index point instead to a shift in behavioral choice, from escape to approach, in hungry animals. We interpret these findings in the framework of risk taking and decision making; feeding state appears to control the propensity to take risks in foraging-related decisions.

On the other hand, we observed a decrease of behavioral responses when starved larvae encountered medium-sized (10°) circles (reduced avoidance, as revealed by a lower activity index and unchanged valence index in Figures 1D and 1E). This difference likely highlights the presence of multiple behavioral components that are modulated by feeding state. 10° circles are too large to be considered as food (Semmelhack et al., 2014) and may be at the threshold of what is considered as a potential threat. These results may, therefore, indicate that hunger reduces predator vigilance, since escapes are energetically costly (Bednekoff, 2007). These two types of modulation are likely evolutionary adaptations allowing fine-tuning of the animal's foraging strategy in response to a variable supply of food resources in the environment.

We showed that starvation decreases aversive behavior by inhibiting the HPI axis. Fed fish have higher levels of cortisol, and a genetic mutation enhancing HPI axis activity is sufficient to mimic the effect of food intake on behavioral choice. Our results are compatible with studies in rodents showing that both rewarding and aversive stimuli are able to activate the HPA axis (Koolhaas et al., 2011). Moreover, in humans and other

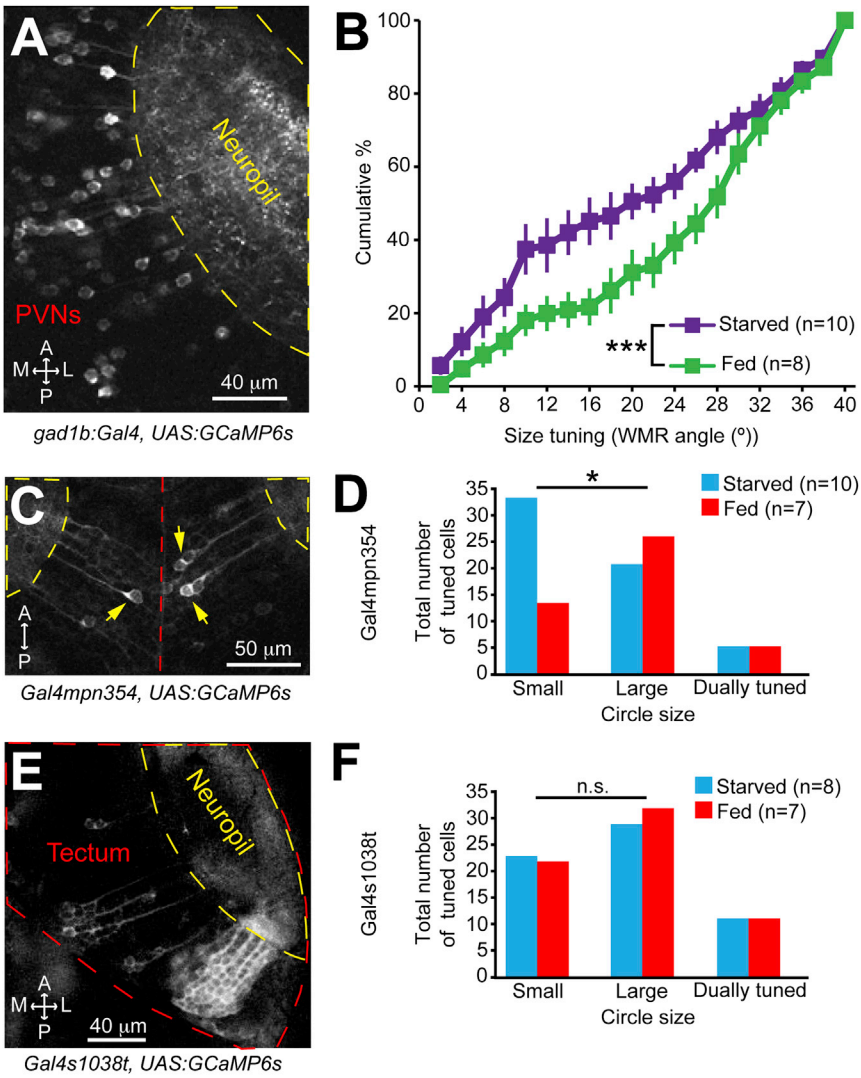

Figure 6. Feeding State Affects the Activity of Specific Populations of Neurons in the Tectum

(A) Two-photon image showing GABAergic neurons in the tectum of a 7 dpf *gad1b:Gal4, UAS:GCaMP6s* larva.

(B) Graph comparing cumulative percentages of WMR angles for tectal GABAergic neurons in starved and fed 7 dpf *gad1b:Gal4, UAS:GCaMP6s* larvae. ***p = 3.9E−5, two-sample Kolmogorov-Smirnov test. Data are presented as mean ± SEM.

(C) Two-photon image showing part of the tectum of a 6 dpf *Gal4mpn354, UAS:GCaMP6s* larva. The red and yellow dashed lines mark the brain midline and tectal neuropils, respectively.

(D) Graph showing numbers of *Gal4mpn354* cells tuned to small (≤10°) or large (≥20°) visual stimuli. Dually tuned neurons responded to both small and large stimuli. Examples of the three types of responses are shown in Figure S3. *p = 0.02, Fisher's exact test.

(E) Two-photon image showing part of the tectum of a 7 dpf *Gal4s1038t, UAS:GCaMP6s* larva.

(F) Plot showing numbers of *Gal4s1038t* neurons tuned to visual stimuli of different sizes in starved and fed animals. n.s., not significant, Fisher's exact test.

A, anterior; L, lateral; M, medial; P, posterior; PVN, peri-ventricular neuron.

See also Figure S3.

mammals, activation of the HPA axis is similarly accompanied by a shift from flexible, goal-directed behaviors, like food seeking in this study, to more rigid stimulus-response behaviors (i.e., escape) (Hermans et al., 2014). More work will be required to pinpoint the exact elements of the HPI axis involved in this type of modulation. CRH is a likely candidate (Fox and Lowry, 2013). However, the GR itself may also be involved, since the $gr^{s357/s357}$ fish combine a gain of function (over-activation) of the HPI axis with a loss of transcriptional function of the GR (Ziv et al., 2013).

Serotonin is a neuromodulator capable of dramatically influencing behavior (Dayan and Huys, 2009). Our results demonstrate that starvation increases the activity of serotonergic neurons in the raphe nucleus, one of the most prominent serotonergic centers in the vertebrate brain (Abrams et al., 2004), and that activation of the serotonergic system is capable of mediating the modulatory action of starvation on behavioral choice in larval zebrafish. Serotonin likely acts downstream of signals from the HPI axis, as shown by studies in rodents where, for example, CRH inhibits serotonergic neurons in the dorsal raphe nucleus (Fox and Lowry, 2013).

Importantly, our findings demonstrate that feeding state modulates information processing at early stages of the visual pathway. In hungry larvae, a greater number of tectal PVNs responded to small, prey-like, visual objects. That food-like items are overrepresented in the tectum of starved fish is consonant with studies in primates, which suggested that relevant information is selected by top-down modulation of neural activity in early sensory areas (Baluch and Itti, 2011). We found that this shift could be explained, at least in part, by changes in GABAergic responses. In starved fish, more GABAergic neurons were activated by small visual stimuli. These could, in turn, suppress aversive behavior (Brandão et al., 2005). Alternatively, the increase in GABAergic responses might serve to balance any increase in excitatory tone. The identification of specialized types of GABAergic neurons will be required to distinguish between these possibilities. Interestingly, we found that a subpopulation of PVNs, labeled in the gene-trap line *Gal4mpn354* and previously implicated in biasing the choice to approach small visual stimuli (Barker and Baier, 2015), are also modulated by feeding state. On the other hand, feeding state did not alter the activity of a different population of tectal neurons, labeled in the enhancer-trap line *Gal4s1038t* and not involved in this particular behavior (Barker and Baier, 2015). Together, the data presented here and previously by Barker and Baier

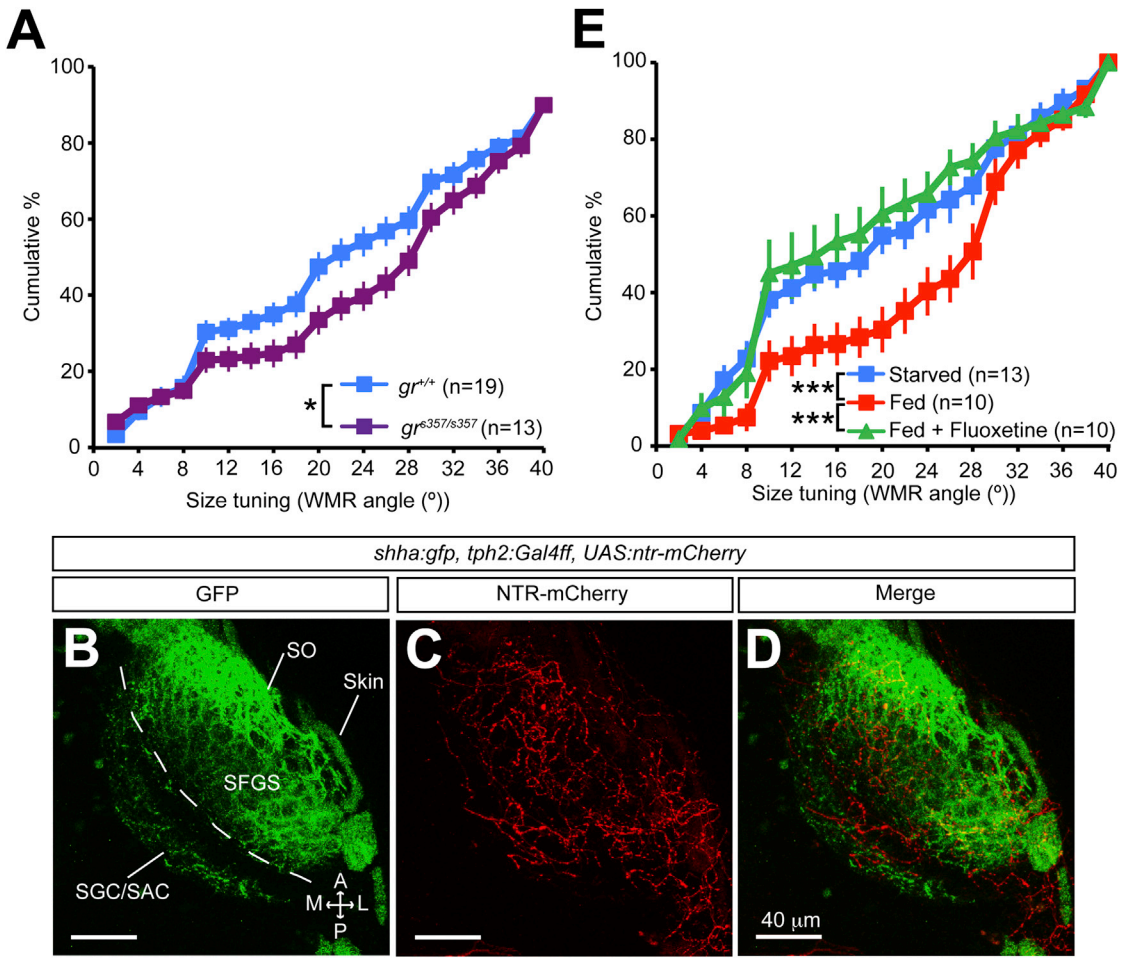

Figure 7. The HPI Axis and the Serotonergic System Modulate Visual Information Processing in the Tectum

(A) Graph depicting cumulative percentages of WMR angles for PVNs in starved 7 dpf *elavl3:Gal4, UAS:GCaMP5, gr*$^{s357/s357}$ and starved control *elavl3:Gal4, UAS:GCaMP5, gr*$^{+/+}$ larvae. *p = 0.02, two-sample Kolmogorov-Smirnov test.

(B–D) Confocal images of a 7 dpf *shha:gfp, tph2:Gal4ff, UAS:ntr-mCherry* larva showing the presence of serotonergic innervation (red neurites in C and D) in the tectum neuropil (GFP-positive RGC axons in B and D). A, anterior; L, lateral; M: medial; NTR, nitroreductase; P, posterior; SAC, stratum album centrale; SFGS, stratum fibrosum et griseum superficiale; SGC, stratum griseum centrale; SO, stratum opticum.

(E) Graph comparing average cumulative percentages of WMR angles for PVNs of fed *elavl3:Gal4, UAS:GCaMP5* larvae treated with 1.5 µM fluoxetine and untreated fed or starved controls. Fluoxetine abolished the satiety-induced change of PVN population response. ***p < 0.001, two-sample Kolmogorov-Smirnov tests. Data are presented as mean ± SEM.

(2015), suggest that feeding state may influence behavioral decisions by modulation of a small population of tectal neurons.

We did not detect macroscopic presynaptic effects of feeding state on retinotectal synaptic transmission. This suggests that the action of feeding state on visual stimulus processing affects postsynaptic functions of downstream PVNs. Alternatively, a small population of RGCs specialized for detection of food or predator-like stimuli (Semmelhack et al., 2014), unnoticeable in our assay, could also be altered. The identification of genetic markers capable of driving expression of transgenes in such populations of RGCs will be required to rule out this possibility.

We showed that the modulation of feeding state on visual processing is mediated by the HPI axis and the serotonergic system. Activation of the HPI axis induced a shift of visual responses similar, although smaller, than that caused by satiation. On the other hand, enhancing serotonergic transmission abolished the effect of food intake on tectal visual processing. These results agree with previous studies, which revealed a central role for the serotonergic system in controlling the processing of sensory inputs (Hurley et al., 2004).

Modulatory effects of serotonin are notoriously complex. By a combination of selective connectivity and differential expression of receptors with opposing properties, serotonin is able to differentially change the activity of individual circuit elements. The mechanisms of action may involve repression or activation of discrete populations of neurons tuned to specific stimulus properties or altering the tuning of neurons (Hurley et al., 2004; Xiang and Prince, 2003). Our data suggest that serotonin mediates the modulation of hunger on visual processing by recruiting additional PVNs responsive to small visual stimuli,

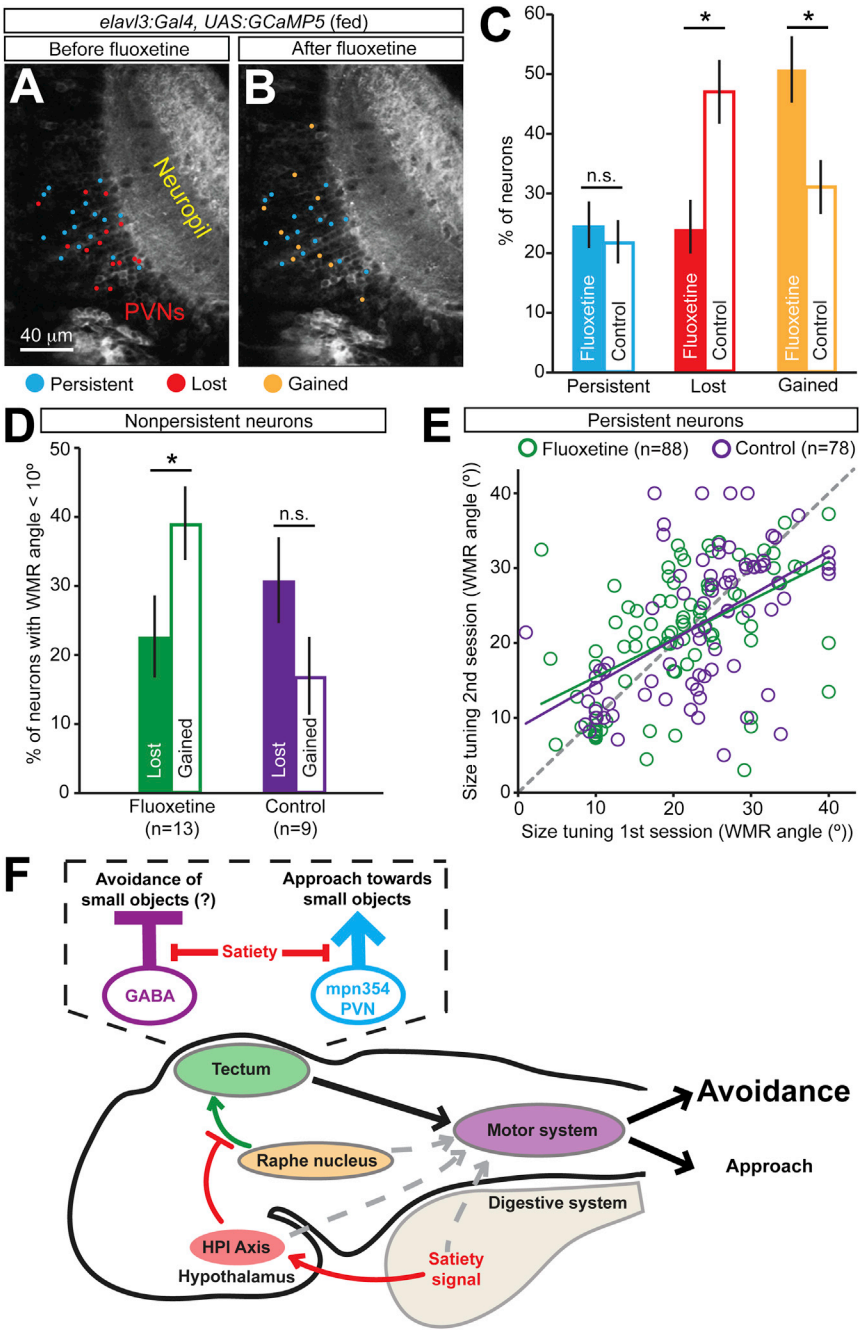

Figure 8. Serotonin Activates a Population of Tectal Neurons Tuned to Small Visual Stimuli in Fed Larvae

(A and B) Two-photon images of a tectum of a fed 7 dpf *elavl3:Gal4, UAS:GCaMP5* larva before (A) and after (B) application of 1.5 μM fluoxetine for 3.5–4 hr. PVN, peri-ventricular neuron.

(C) Bar graph showing the average percentages of neurons active only in the first (lost) or second (gained) recording session, or at both times (persistent). In the first session, fed 7 dpf *elavl3:Gal4, UAS:GCaMP5* larvae were imaged. In the second session, the same animals were imaged again in the absence (control group) or presence of fluoxetine. *$p < 0.04$; n.s., not significant (t test with Benjamini-Hochberg correction). n = 13 (fluoxetine) and 9 (control) larvae.

(D) Average percentages of nonpersistent neurons (corresponding to the "lost" and "gained" groups in C) tuned to small-sized visual stimuli. *$p = 0.05$, paired t test. Error bars represent SEM.

(E) Scatterplot displaying WMR angles of persistent neurons in the first and second imaging sessions. Each circle represents a neuron. No statistically significant differences between the two groups were detected ($p = 1$, ANOVA). n = number of neurons. The green and purple lines represent linear regressions of the data relative to the fluoxetine-treated ($r^2 = 0.26$) and control ($r^2 = 0.27$) group, respectively. The dashed gray line marks the position occupied by data points relative to neurons whose response properties were the same in the two imaging sessions.

(F) Scheme summarizing the results. A satiety signal, potentially from the digestive system, activates the HPI axis, which, in turn, inhibits serotonergic neurons in the raphe nucleus sending axons to the tectum. Satiety may alter visuomotor transformations in the tectum in at least two ways (inset). First, it may increase avoidance of small objects by inhibiting a population of GABAergic neurons responsive to small- and medium-sized visual stimuli. Second, it decreases pursuit of small objects by inhibiting *mpn354* PVNs. This modulation biases downstream motor circuits toward avoidance of small- and medium-sized objects. Additional fine-tuning by feeding state of other neural circuits could also contribute to the final behavioral choice (gray dashed arrows).

without significantly altering the size tuning of individual tectal neurons.

Taken together, our data suggest a model in which starvation, by inhibiting the HPI axis and enhancing serotonergic transmission, alters visual-motor transformations in the tectum, most likely through the activation of specific populations of neurons capable of biasing behavioral choice (Figure 8F). Such a modulation of visual information processing, possibly together with the fine-tuning of other neural circuits, could help an animal to choose an adaptive behavioral output in the face of ambiguous environmental stimuli.

EXPERIMENTAL PROCEDURES

Zebrafish Maintenance and Care

Fish were raised and bred at 28°C on a 14 hr/10 hr light/dark cycle. Embryos and larvae were raised in Danieau's medium (58 mM NaCl, 0.7 mM KCl, 0.4 mM $MgSO_4$, 0.6 mM $Ca(NO_3)_2$, 5 mM HEPES, and 0.5 mg/l methylene blue [pH 7.6]). All animal procedures were approved by the local government authorities (Regierung Oberbayern).

Zebrafish Lines

The transgenic lines *Tg(Shha:GFP)t10* (Neumann and Nuesslein-Volhard, 2000; RRID: ZFIN_ZDB-GENO-060207-1), *Tg(elavl3:Gal4-VP16)nns6* (Kimura

et al., 2008), *Tg(tph2:Gal4ff)y228* (Yokogawa et al., 2012; RRID: ZFIN_ZDB-GENO-121114-19), *Tg(Gal4mpn354)* (Barker and Baier, 2015), *Et(Gal4-VP16)s1038t* (Scott et al., 2007; RRID: ZFIN_ZDB-GENO-110912-8), *Tg(isl2b:Gal4-VP16)zc60* (Ben Fredj et al., 2010; RRID: ZFIN_ZDB-GENO-150320-5), *Tg(UAS:GCaMP5)zf352* (Akerboom et al., 2012), *Tg(UAS:GCaMP6s)mpn101* (Thiele et al., 2014; RRID: ZFIN_ZDB-GENO-140811-5), *Tg(UAS:GFP)mpn100* (Thiele et al., 2014; RRID: ZFIN_ZDB-GENO-140812-1), and *Tg(UAS:ntr-mCherry)c264* (Davison et al., 2007; RRID: ZFIN_ZDB-GENO-070316-1) were previously reported. The transgenic line *Tg(gad1b:Gal4VP16)mpn155* was generated by inserting a DNA fragment containing a *Gal4VP16* sequence and a *myl7:mCherry* (bleeding heart) cassette downstream of the *gad1b* promoter in a bacterial artificial chromosome (BAC) (clone #CH211-24M22), using standard recombineering and *Tol2*-mediated transgenesis techniques (Bussmann and Schulte-Merker, 2011).

Zebrafish harboring the gr^{s357} mutation (RRID: ZFIN_ZDB-GENO-121109-4) were identified in a forward genetic screen (Muto et al., 2005; Ziv et al., 2013). Larvae for the experiments were obtained by incrossing $gr^{+/s357}$ heterozygous fish. Genotyping was carried out by sequencing the PCR product generated with primers flanking the genomic region containing the point mutation (forward: 5′-AATTACCTGTGTGCTGGGCGAAAC-3′, reverse: 5′-CTCAGTTTATC CACATTTATGCAGCTC-3′).

The majority of the experiments were performed with Tüpfel long-fin (TL) zebrafish. Fish harboring the gr^{s357} mutation had a mixed TL/WIK genetic background. *Tg(tph2:Gal4ff)y228* fish were a mix of TL and an unknown strain.

Feeding Protocol

Zebrafish larvae were divided in two groups at 6 dpf in 9 cm Petri dishes containing Danieau's solution. One group was provided with food powder (sera Micron; sera), while the other one was not fed. The medium and food were changed at 7 dpf, ~4 hr before experiments were carried out. Larvae of both groups received equal number and timing of transfers. Potential changes of physicochemical properties of the Danieau's solution due to the presence of the food were monitored by measuring the pH and osmolarity with a glass electrode pH meter or a freezing point osmometer, respectively. pH and osmolarity of the solutions were found to be similar in the two groups (Table S1). From the fed group, only larvae containing food in their digestive tract were selected for experiments (Figure 1C).

To prepare the odor solution used for the experiments described in Figure 4F, food powder was added to Danieau's medium. The resulting suspension was vortexed for 10 min, centrifuged for 3 min at 3,000 rpm, and then filtered with a 0.22 μm syringe filter. The odor solution was applied instead of food to zebrafish larvae, with the same modalities and timing described earlier.

Larvae were washed in Danieau's medium to remove food residue or odor solution before performing experiments. All experiments were performed in the afternoon.

Behavioral Assay

The size discrimination assay was described previously (Barker and Baier, 2015). A single zebrafish larva was placed in a transparent plastic chamber containing Danieau's solution, under which a computer screen displayed arrays of moving black circles on a white background with a constant speed of 42°/s. Nine circles of each size were presented for 30 s in each of five trials. The durations of larva-stimulus interactions were variable, owing to the fact that fish were not physically restrained. Representative examples of larva-stimulus interactions are shown in Movies S1 and S2. Visual stimuli were created in MATLAB using Psychtoolbox (Brainard, 1997). Circle sizes were calculated as the degrees of the visual field, occupied by the stimulus positioned right below a larva, and ranged from 1° to 50°. Since the larvae were unrestrained, the actual circle size at which each larva-circle interaction occurred was an approximate estimation, and we reported the size of each circle as a means of distinguishing between the relative sizes of the visual stimuli. Videos were recorded with a camera above the chamber at 60 frames per second.

Each larva-circle interaction was scored either as an approach or an avoidance when the fish swam toward or away from a moving circle, respectively (Barker and Baier, 2015). Neutral interactions were scored when fish neither approached nor avoided moving circles. A valence index [VI; (approaches − avoidances)/(approaches + avoidances)] was calculated to quantify the tendency of fish to approach or avoid circles. VI = 1 with 100% approach and −1 with 100% avoidance. An activity index [AI; (approaches + avoidances)/(approaches + avoidances + neutral interactions)] was calculated to quantify the general efficiency of larva-circle interactions. AI = 0 with 100% neutral interactions and 1 with 0% neutral interactions. The behavior was scored by an observer blinded to the identities of the experimental groups.

$gr^{s357/s357}$ mutant larvae analyzed with this behavioral assay were identified on the basis of impaired visual background adaptation (Muto et al., 2005), and the genotype of the majority of fish was also confirmed by DNA sequencing as described earlier.

Two-Photon Calcium Imaging and Data Analyses

7 dpf larvae were embedded in 2% low-melting-point agarose and imaged with a movable-objective two-photon microscope (MOM; Sutter Instrument) equipped with a mode-locked titanium:sapphire Chameleon UltraII laser (Coherent) tuned to 920 nm and controlled by ScanImage software (Pologruto et al., 2003). The image acquisition rate was 3.37 Hz. Visual stimuli (black circles, ranging from 1° to 40° of the visual field, moving on a gray background) were generated using a custom program in Vision Egg software (Straw, 2008) and presented with an 800-pixel × 600-pixel OLED microdisplay (eMagin) with two green light-blocking filters to the left eye of the larvae. Imaging was performed in the right (contralateral) tectum. Image time series, when necessary, were x-y motion-corrected, either with an algorithm written in MATLAB (Dombeck et al., 2007) or with the StackReg Fiji plugin, and analyzed with Fiji (Schindelin et al., 2012).

The larvae used for imaging were TLN ($mitfa^{-/-}$) mutants lacking skin melanophores (Lister et al., 1999). For imaging activity of tectal PVNs, *Tg(elavl3:Gal4), Tg(UAS:GCaMP5)zf352* larvae were used. For the experiments described in Figure 8, 7 dpf *Tg(elavl3:Gal4), Tg(UAS:GCaMP5)zf352* larvae were incubated in 1.5 μM fluoxetine dissolved in Danieau's medium (or only Danieau's medium for controls) for 3.5–4 hr after the first imaging session. 7 dpf *Tg(gad1b:Gal4VP16)mpn155, Tg(UAS:GCaMP6s)mpn101* larvae were used for imaging activity of tectal GABAergic neurons. Analysis of calcium signals was performed with Fiji. Regions of interest (ROIs) were selected manually based on the presence of an increase of GCaMP5 fluorescence correlated with visual stimulus presentations. ΔF/F values were calculated as $(F_t - F_0)/F_0$, where F_t is the fluorescence at time t and F_0 is the baseline fluorescence, defined as the average fluorescence of the nine frames preceding the first stimulus. Signal detection threshold was set as twice the standard deviation of the baseline. WMR angles were calculated as weighted sums of visual stimulus sizes, to which Ca^{2+} responses were non-zero:

$$WMRangle = \sum_{i=1}^{n} w_i x_i$$

where x_i are the angular sizes of the visual stimuli and w_i are the weights calculated as

$$w_i = \frac{(\Delta F/F)_i}{\sum_{i=1}^{n} (\Delta F/F)_i}.$$

For imaging activity in RGC axons, 7 dpf *Tg(isl2b:Gal4-VP16), Tg(UAS:GCaMP6s)mpn101* larvae were used. The pixel-wise analysis of the responses in the tectal neuropil was performed with a regression-based identification of the size tuning (Miri et al., 2011). Briefly, the temporal series for each pixel in the field of view were represented by a linear regression model with a basis composed of seven independent variables, corresponding to the individual responses for the different sizes, and by a constant term. These regressor functions were obtained from the convolution of the waveforms of the stimulus presence with a GCaMP6s kernel, whose τ_{off} = 1.8 s was based on the coefficient of determination R^2. From the resulting set of coefficients, the distributions of T scores for different sizes and conditions were averaged across different trials. Corrected distributions were obtained subtracting a component corresponding to the recording done in absence of visual stimuli. The integrals of the corrected distributions were used for quantifying the amount

of pixels activated by the presentation of visual stimuli of different sizes (Figure 5C).

Imaging of *Tg(Gal4mpn354), Tg(UAS:GCaMP6s)mpn101* larvae was performed at 6 and 7 dpf. *Et(Gal4-VP16)s1038t, Tg(UAS:GCaMP6s)mpn101* fish were imaged at 7 dpf. *Z* scores were calculated for the average calcium response (ΔF/F averaged over two or three trials) for each neuron at each visual stimulus size. If a neuron had a Z score of 1.0 or greater for an individual size, the neuron was considered as "tuned" to that size. Neurons were classified as single tuned if tuned only to small ($\leq 10^{\circ}$) or large ($\geq 20^{\circ}$) visual stimuli. Neurons tuned to both small and large stimuli were classified as dually tuned.

Immunofluorescence Staining and Quantification

7 dpf starved or fed zebrafish larvae were anesthetized and fixed in 4% paraformaldehyde in PBS with 0.3% Triton (PBT) at 4°C overnight. After three 15 min washes in PBT, larvae were incubated in 150 mM Tris-HCl (pH 9) for 5 min at room temperature followed by 15 min at 70°C. Larvae were washed again in PBT before they were incubated in Trypsin EDTA (Sigma-Aldrich #T4299, diluted 1:20 in PBT) on ice. PBT-washed larvae were blocked in 5% goat serum, 1% BSA, and 1% DMSO in PBT for 1 hr at room temperature. Primary antibodies (1:500 dilution) were added in blocking solution for 72–96 hr at 4°C. Larvae were washed again in PBT, and secondary antibodies were added at 1:300 in blocking solution for 48–72 hr at 4°C. Primary antibodies against the following antigens were used: total ERK (tERK; Cell Signaling Technology #4696; RRID: AB_390780), phosphorylated ERK (pERK; Cell Signaling Technology #4370; RRID: AB_2315112), and GFP (Thermo Fisher Scientific #A10262; RRID: AB_2534023). The following Alexa Fluor (AF) secondary antibodies were used: α-chicken-AF488 (Thermo Fisher #A11039; RRID: AB_10563770), α-rabbit-AF546 (Thermo Fisher Scientific #A11010; RRID: AB_10584649), and α-mouse-AF647 (Thermo Fisher Scientific #A21235; RRID: AB_10562370). PBT-washed larvae were embedded in 2% low-melting-point agarose, and confocal images were acquired. Constant acquisition settings were used for imaging all larvae. The intensities of pERK and tERK stainings were quantified as integrated densities in Fiji. Only GFP-positive cells in the raphe nuclei of *Tg(tph2:Gal4ff)y228, Tg(UAS:GFP)mpn100* larvae were selected for the analysis.

Confocal Imaging

Zebrafish larvae were anesthetized with 0.016% tricaine in Danieau's medium and embedded in 2% low-melting-point agarose. Confocal imaging was performed on a Zeiss LSM780 microscope. Image stacks were acquired with 1 μm z-steps.

Drug Treatments

Zebrafish larvae were treated with 1.5 μM fluoxetine hydrochloride (Sigma-Aldrich) dissolved in Danieau's medium starting 4 to 6 hr before behavioral or two-photon calcium imaging experiments. The drug was present in the medium while experiments were carried out.

Nitroreductase-Mediated Cell Ablations

10 mM metronidazole (MTZ) + 1% DMSO in Danieau's solution was applied to 4 dpf *Tg(tph2:Gal4ff)y228, Tg(UAS:ntr-mCherry)c264* larvae and control fish lacking NTR-mCherry expression. MTZ was removed at 6 dpf, and behavioral experiments were performed at 7 dpf. Fish were kept in the dark during MTZ treatment to prevent inactivation of the drug by light exposure. A minority of fish (6.8% of NTR-negative, 27.6% of Gal4- and NTR-double positive larvae) used for experiments displayed low motor activity after MTZ treatment and were not included in the analysis.

Cortisol Measurements

Zebrafish larvae were either provided with or deprived of food according to the feeding protocol described earlier. 7 dpf larvae from each group were pooled in sets of 24 individuals, anesthetized with 0.016% tricaine in Danieau's medium, and lysated with a tissue homogenizer. Cortisol was extracted following a previously described protocol (Yeh et al., 2013). Cortisol amounts were measured using an enzyme immunoassay detection kit (Caymanchem) according to the manufacturer's instructions.

Statistical Analyses

Statistical significance was determined using two-tailed Student's t tests in Microsoft Excel; two-sample Kolmogorov-Smirnov, Mann-Whitney U, and ANOVA tests in MATLAB; and Fisher's exact test in GraphPad Prism 6.0. The Benjamini-Hochberg procedure was used for controlling the false discovery rate in multiple comparisons (Benjamini and Hochberg, 1995). Unless otherwise stated, n indicates the number of larvae used for experiments.

SUPPLEMENTAL INFORMATION

Supplemental Information includes four figures, two tables, and two movies and can be found with this article online at http://dx.doi.org/10.1016/j.neuron.2016.03.014.

AUTHOR CONTRIBUTIONS

Conceptualization, A.F., and H.B.; Methodology, A.F., and H.B.; Investigation, A.F., and A.J.B.; Formal Analysis, A.F., A.J.B., and M.D.M.; Writing – Original Draft, A.F.; Writing – Review & Editing, A.J.B., H.B., and M.D.M.; Funding Acquisition, A.F., A.J.B., and H.B.; Supervision, H.B.

ACKNOWLEDGMENTS

We thank R. Portugues for critical comments on the manuscript. We thank F. Kubo, I. Arnold-Ammer, D. Förster, and the BAC transgenesis team for generating the *gad1b:Gal4VP16* line, and we thank H. Burgess for providing the *tph2:Gal4ff* fish. A.F. was supported by an EMBO long-term postdoctoral fellowship. A.J.B. was supported by an NSF graduate fellowship. This project was funded by the Max Planck Society, the Center for Integrative Protein Science Munich, and the Deutsche Forschungsgemeinschaft (SFB870 Assembly and Function of Neural Circuits, TP B16).

Received: July 31, 2015
Revised: January 27, 2016
Accepted: March 15, 2016
Published: April 14, 2016

REFERENCES

Abrams, J.K., Johnson, P.L., Hollis, J.H., and Lowry, C.A. (2004). Anatomic and functional topography of the dorsal raphe nucleus. Ann. N Y Acad. Sci. *1018*, 46–57.

Akerboom, J., Chen, T.-W., Wardill, T.J., Tian, L., Marvin, J.S., Mutlu, S., Calderón, N.C., Esposti, F., Borghuis, B.G., Sun, X.R., et al. (2012). Optimization of a GCaMP calcium indicator for neural activity imaging. J. Neurosci. *32*, 13819–13840.

Alderman, S.L., and Bernier, N.J. (2009). Ontogeny of the corticotropin-releasing factor system in zebrafish. Gen. Comp. Endocrinol. *164*, 61–69.

Baier, H., and Scott, E.K. (2009). Genetic and optical targeting of neural circuits and behavior–zebrafish in the spotlight. Curr. Opin. Neurobiol. *19*, 553–560.

Baluch, F., and Itti, L. (2011). Mechanisms of top-down attention. Trends Neurosci. *34*, 210–224.

Bargmann, C.I. (2012). Beyond the connectome: how neuromodulators shape neural circuits. BioEssays *34*, 458–465.

Barker, A.J., and Baier, H. (2015). Sensorimotor decision making in the zebrafish tectum. Curr. Biol. *25*, 2804–2814.

Bednekoff, P.A. (2007). Allocation of foraging efforts when danger varies over time. In Foraging, D.W. Stephens, J.S. Brown, and R.C. Ydenberg, eds. (The University of Chicago Press), pp. 305–329.

Ben Fredj, N., Hammond, S., Otsuna, H., Chien, C.-B., Burrone, J., and Meyer, M.P. (2010). Synaptic activity and activity-dependent competition regulates axon arbor maturation, growth arrest, and territory in the retinotectal projection. J. Neurosci. *30*, 10939–10951.

Benjamini, Y., and Hochberg, Y. (1995). Controlling the false discovery rate: a practical and powerful approach to multiple testing. J. R. Stat. Soc. B *57*, 289–300.

Bräcker, L.B., Siju, K.P., Varela, N., Aso, Y., Zhang, M., Hein, I., Vasconcelos, M.L., and Grunwald Kadow, I.C. (2013). Essential role of the mushroom body in context-dependent CO2 avoidance in Drosophila. Curr. Biol. *23*, 1228–1234.

Brainard, D.H. (1997). The psychophysics toolbox. Spat. Vis. *10*, 433–436.

Brandão, M.L., Borelli, K.G., Nobre, M.J., Santos, J.M., Albrechet-Souza, L., Oliveira, A.R., and Martinez, R.C. (2005). Gabaergic regulation of the neural organization of fear in the midbrain tectum. Neurosci. Biobehav. Rev. *29*, 1299–1311.

Bussmann, J., and Schulte-Merker, S. (2011). Rapid BAC selection for tol2-mediated transgenesis in zebrafish. Development *138*, 4327–4332.

Davison, J.M., Akitake, C.M., Goll, M.G., Rhee, J.M., Gosse, N., Baier, H., Halpern, M.E., Leach, S.D., and Parsons, M.J. (2007). Transactivation from Gal4-VP16 transgenic insertions for tissue-specific cell labeling and ablation in zebrafish. Dev. Biol. *304*, 811–824.

Dayan, P., and Huys, Q.J.M. (2009). Serotonin in affective control. Annu. Rev. Neurosci. *32*, 95–126.

Dombeck, D.A., Khabbaz, A.N., Collman, F., Adelman, T.L., and Tank, D.W. (2007). Imaging large-scale neural activity with cellular resolution in awake, mobile mice. Neuron *56*, 43–57.

Ewert, J.-P. (1970). Neural mechanisms of prey-catching and avoidance behavior in the toad (Bufo bufo L.). Brain Behav. Evol. *3*, 36–56.

Fox, J.H., and Lowry, C.A. (2013). Corticotropin-releasing factor-related peptides, serotonergic systems, and emotional behavior. Front. Neurosci. *7*, 169.

Gahtan, E., Tanger, P., and Baier, H. (2005). Visual prey capture in larval zebrafish is controlled by identified reticulospinal neurons downstream of the tectum. J. Neurosci. *25*, 9294–9303.

Griffiths, B.B., Schoonheim, P.J., Ziv, L., Voelker, L., Baier, H., and Gahtan, E. (2012). A zebrafish model of glucocorticoid resistance shows serotonergic modulation of the stress response. Front. Behav. Neurosci. *6*, 68.

Hermans, E.J., Henckens, M.J.A.G., Joëls, M., and Fernández, G. (2014). Dynamic adaptation of large-scale brain networks in response to acute stressors. Trends Neurosci. *37*, 304–314.

Hirayama, K., and Gillette, R. (2012). A neuronal network switch for approach/avoidance toggled by appetitive state. Curr. Biol. *22*, 118–123.

Hurley, L.M., Devilbiss, D.M., and Waterhouse, B.D. (2004). A matter of focus: monoaminergic modulation of stimulus coding in mammalian sensory networks. Curr. Opin. Neurobiol. *14*, 488–495.

Inagaki, H.K., Panse, K.M., and Anderson, D.J. (2014). Independent, reciprocal neuromodulatory control of sweet and bitter taste sensitivity during starvation in Drosophila. Neuron *84*, 806–820.

Kahneman, D., and Tversky, A. (1979). Prospect theory: An analysis of decision under risk. Econometrica *47*, 263–291.

Kimmel, C.B., Ballard, W.W., Kimmel, S.R., Ullmann, B., and Schilling, T.F. (1995). Stages of embryonic development of the zebrafish. Dev. Dyn. *203*, 253–310.

Kimura, Y., Satou, C., and Higashijima, S. (2008). V2a and V2b neurons are generated by the final divisions of pair-producing progenitors in the zebrafish spinal cord. Development *135*, 3001–3005.

Koolhaas, J.M., Bartolomucci, A., Buwalda, B., de Boer, S.F., Flügge, G., Korte, S.M., Meerlo, P., Murison, R., Olivier, B., Palanza, P., et al. (2011). Stress revisited: a critical evaluation of the stress concept. Neurosci. Biobehav. Rev. *35*, 1291–1301.

Kristan, W.B., Jr. (2008). Neuronal decision-making circuits. Curr. Biol. *18*, R928–R932.

Lima, S.L., and Dill, L.M. (1990). Behavioral decisions made under the risk of predation: a review and prospectus. Can. J. Zool. *68*, 619–640.

Lister, J.A., Robertson, C.P., Lepage, T., Johnson, S.L., and Raible, D.W. (1999). nacre encodes a zebrafish microphthalmia-related protein that regulates neural-crest-derived pigment cell fate. Development *126*, 3757–3767.

Löhr, H., and Hammerschmidt, M. (2011). Zebrafish in endocrine systems: recent advances and implications for human disease. Annu. Rev. Physiol. *73*, 183–211.

Longden, K.D., Muzzu, T., Cook, D.J., Schultz, S.R., and Krapp, H.G. (2014). Nutritional state modulates the neural processing of visual motion. Curr. Biol. *24*, 890–895.

Marella, S., Mann, K., and Scott, K. (2012). Dopaminergic modulation of sucrose acceptance behavior in Drosophila. Neuron *73*, 941–950.

Miri, A., Daie, K., Burdine, R.D., Aksay, E., and Tank, D.W. (2011). Regression-based identification of behavior-encoding neurons during large-scale optical imaging of neural activity at cellular resolution. J. Neurophysiol. *105*, 964–980.

Muto, A., Orger, M.B., Wehman, A.M., Smear, M.C., Kay, J.N., Page-McCaw, P.S., Gahtan, E., Xiao, T., Nevin, L.M., Gosse, N.J., et al. (2005). Forward genetic analysis of visual behavior in zebrafish. PLoS Genet. *1*, e66.

Neumann, C.J., and Nuesslein-Volhard, C. (2000). Patterning of the zebrafish retina by a wave of sonic hedgehog activity. Science *289*, 2137–2139.

Nevin, L.M., Robles, E., Baier, H., and Scott, E.K. (2010). Focusing on optic tectum circuitry through the lens of genetics. BMC Biol. *8*, 126.

Niell, C.M., and Smith, S.J. (2005). Functional imaging reveals rapid development of visual response properties in the zebrafish tectum. Neuron *45*, 941–951.

Palmer, C.R., and Kristan, W.B., Jr. (2011). Contextual modulation of behavioral choice. Curr. Opin. Neurobiol. *21*, 520–526.

Pearson, J.M., Watson, K.K., and Platt, M.L. (2014). Decision making: the neuroethological turn. Neuron *82*, 950–965.

Pisharath, H., Rhee, J.M., Swanson, M.A., Leach, S.D., and Parsons, M.J. (2007). Targeted ablation of beta cells in the embryonic zebrafish pancreas using E. coli nitroreductase. Mech. Dev. *124*, 218–229.

Pologruto, T.A., Sabatini, B.L., and Svoboda, K. (2003). ScanImage: flexible software for operating laser scanning microscopes. Biomed. Eng. Online *2*, 13.

Preuss, S.J., Trivedi, C.A., vom Berg-Maurer, C.M., Ryu, S., and Bollmann, J.H. (2014). Classification of object size in retinotectal microcircuits. Curr. Biol. *24*, 2376–2385.

Randlett, O., Wee, C.L., Naumann, E.A., Nnaemeka, O., Schoppik, D., Fitzgerald, J.E., Portugues, R., Lacoste, A.M.B., Riegler, C., Engert, F., and Schier, A.F. (2015). Whole-brain activity mapping onto a zebrafish brain atlas. Nat. Methods *12*, 1039–1046.

Rosen, L.B., Ginty, D.D., Weber, M.J., and Greenberg, M.E. (1994). Membrane depolarization and calcium influx stimulate MEK and MAP kinase via activation of Ras. Neuron *12*, 1207–1221.

Schindelin, J., Arganda-Carreras, I., Frise, E., Kaynig, V., Longair, M., Pietzsch, T., Preibisch, S., Rueden, C., Saalfeld, S., Schmid, B., et al. (2012). Fiji: an open-source platform for biological-image analysis. Nat. Methods *9*, 676–682.

Scott, E.K., Mason, L., Arrenberg, A.B., Ziv, L., Gosse, N.J., Xiao, T., Chi, N.C., Asakawa, K., Kawakami, K., and Baier, H. (2007). Targeting neural circuitry in zebrafish using GAL4 enhancer trapping. Nat. Methods *4*, 323–326.

Semmelhack, J.L., Donovan, J.C., Thiele, T.R., Kuehn, E., Laurell, E., and Baier, H. (2014). A dedicated visual pathway for prey detection in larval zebrafish. eLife *3*, e04878.

Straw, A.D. (2008). Vision egg: an open-source library for realtime visual stimulus generation. Front. Neuroinform. *2*, 4.

Symmonds, M., Emmanuel, J.J., Drew, M.E., Batterham, R.L., and Dolan, R.J. (2010). Metabolic state alters economic decision making under risk in humans. PLoS ONE *5*, e11090.

Temizer, I., Donovan, J.C., Baier, H., and Semmelhack, J.L. (2015). A visual pathway for looming-evoked escape in larval zebrafish. Curr. Biol. *25*, 1823–1834.

Thiele, T.R., Donovan, J.C., and Baier, H. (2014). Descending control of swim posture by a midbrain nucleus in zebrafish. Neuron *83*, 679–691.

Ulrich-Lai, Y.M., and Herman, J.P. (2009). Neural regulation of endocrine and autonomic stress responses. Nat. Rev. Neurosci. *10*, 397–409.

Xiang, Z., and Prince, D.A. (2003). Heterogeneous actions of serotonin on interneurons in rat visual cortex. J. Neurophysiol. *89*, 1278–1287.

Yeh, C.-M., Glöck, M., and Ryu, S. (2013). An optimized whole-body cortisol quantification method for assessing stress levels in larval zebrafish. PLoS ONE *8*, e79406.

Yokogawa, T., Hannan, M.C., and Burgess, H.A. (2012). The dorsal raphe modulates sensory responsiveness during arousal in zebrafish. J. Neurosci. *32*, 15205–15215.

Ziv, L., Muto, A., Schoonheim, P.J., Meijsing, S.H., Strasser, D., Ingraham, H.A., Schaaf, M.J.M., Yamamoto, K.R., and Baier, H. (2013). An affective disorder in zebrafish with mutation of the glucocorticoid receptor. Mol. Psychiatry *18*, 681–691.